

Early Tumor Detection by Multiple Infrared Unsupervised Neural Nets Fusion

Harold Szu^{1,2}, Ivica Kopriva¹, Philip Hoekstra³, Nicholas Diakides⁴, Mary Diakides⁴, James Buss², and Jasper Lupo

¹Digital Media RF Lab, 725 23rd St. NW, Lab 308, Dept. ECE, GWU, Wash. DC 20052;

²ONR Code 313 Sensors & Surveillance, 800 NQ St., Arlington, VA 22217-5660;

³Thermal Scan Inc., Michigan; ⁴Advanced Concepts Analysis, Inc., 6353 Crosswoods Drive, Falls Church, VA 22044

Abstract- The unsupervised classification algorithm called Lagrange Constraint Neural Network (LCNN) has been successfully applied to the sub-pixel multi-spectral remote sensing, [25]. Here, we apply the LCNN to the early breast cancer detection using two-color mid and long infrared images of the breast. This could be a new paradigm shift that enabled smart neural network algorithm to sort out the underlying malignant heat sources for physician diagnoses. The non-intrusive 2-color passive infrared imaging that could be repeated for record track with no radiation hazard seems to be alternative paradigm shift for the first-line screening against breast cancer. The sub-pixel super-resolution capability of the remote sensing is equivalent to the sub-millimeter scaling of the close-up breast imaging for the vascular and the angiogenesis effects. We demonstrate the potential benefit of the multi-color mid & long infrared imaging capable for detecting the abnormal under-skin thermal textures as well as stage-zero detection of the ductal carcinoma in situ.

I. INTRODUCTION

Early detection of the breast cancer should result in the increased survival probability. Decades data seemed to breed statistical controversial of the X-ray mammogram [19]. On the other hand, the cost-effective thermal infrared imaging in single spectral band has been routinely applied [21, 22] and established screening tool in breast cancer [20] in developed countries in Europe as well as in developing countries in Asia due to the fear of the X-ray radiation hazard. In this paper, we applied brain-like smart neural network algorithm that demanded an eye-like pair of IR sensors. To promote both convenient and effective diagnoses, we recommend application of the smart sub-pixel super-resolution multiple spectral remote sensing algorithm called Lagrange Constraint neural Network (LCNN) [23-25] to the multiple spectral band breast imageries. We recapitulate Keyserlink et al. [18] review of IR breast imaging. In 1961 Williams and Handley [1], using a rudimentary handheld thermopile, reported that 54 out of 57 of their breast cancer patients were detectable by IR imaging, and "among these were cases in which the clinical diagnosis was in much doubt". In 1962, Handley [2] demonstrated a close correlation between the increased thermal pattern and increased recurrence rate. In 1963, Lawson and Chughtai [3] demonstrated that increase in the regional temperature associated with the breast cancer was related to venous convection. In 1965, Gershen-Cohen [4] introduced IR imaging to the United States reporting 4000 described in Section III while brief conclusion is given in Section IV.

cases with a remarkable true positive rate of 94% and false positive rate of 6%. Keyserlink, Habreman, and Jones improved such an ROC curve, [4-7]. In 1972, Dodd [8] concluded that IR imaging would eliminate 80 to 85% of the potential mammograms. Wallace [10] presented an update on IR imaging that poses no radiation burden on the patient; requires no physical contact; and, being an innocuous technique, could concentrate the sought population by a significant factor, selecting those patients that required further investigation. However, despite newly available military IR technology, as well as compelling statistics of 70,000 cases [18], the acceptance of passive IR imaging in the US was not comparable with the active X-ray mammography. This was surprising from the current consensus standpoint regarding vascular-related tumor initiation and growth that provided a plausible explanation for the IR finding. In 1993, Head and Elliott [12] improved images of the high resolution second-generation IR systems provided objective and quantitative analysis, and reported that the growth-rate-related prognostic indicators were strongly associated with the IR results [13]. In 1996, Gamagami [14] studied angiogenesis by IR imaging and reported that hypervascularity and hyperthermia could be shown in 86% of non-palpable breast cancers. He also noted that in 15% of these cases, this technique helped to detect cancers that were not visible through mammography. The concept of angiogenesis, suggested by Gamagami as an integral part of early breast cancer, was reiterated in 1996 by Guido and Schnitt [15], whose observations suggested that angiogenesis is an early event in the development of breast cancer. They noted that it might occur before tumor cells acquired the ability to invade the surrounding stoma and even before there was morphologic evidence of a ductal carcinoma in situ (DCIS). Anbar [16, 17] suggested, using an elegant biochemical and immunological cascade, the empirical observation that small tumors capable of producing notable IR changes could be due to enhanced perfusion over a substantial area of breast surface via tumor-induced nitric oxide vasodilatation. He introduced the importance of dynamic area tele-thermometry to validate IR's full potential. We proposed in Section II to reassess currently available IR technology, spearheaded by the military R/D multispectral remote sensing to the breast cancer. The experimental results are described in Section III. Brief conclusion is given in Section IV.

II. BRAIN-LIKE LCNN REQUIRED PAIR OF SENSORS

To promote convenient and effective diagnoses, we recommend application of the sub-pixel multi-spectral algorithm coined Lagrange Constraint Neural Network (LCNN) [23-25] to the multispectral IR images of the breast. LCNN algorithm solves blind image de-mixing problem on the pixel-by-pixel basis at the minimum of the Helmholtz free energy. That enables LCNN algorithm to compute the sub-pixel super-resolution in a massively pixel parallel (MPP) manner. It has been demonstrated in [25] how application of the LCNN algorithm to blind de-mixing of the LANDSAT 7 multispectral data can detect small man-made structures in the desert. Motivated by that result we propose application of described multispectral LCNN algorithm to the multi-color IR breast imagery for early cancer detection.

III. PRELIMINARY EXPERIMENTAL RESULTS

The LCNN algorithm has been applied to de-mix two-color mid and long wave IR breast images shown on Figure 1. The breast thermograms were taken from the same person, in the same room, under the same circumstances with a medium wave (Cincinnati Electronics Iris 256 LN Indium Antimonide 3-5 micrometer) camera and a long wave (ICC, MBC 200 Platinum Selicide 9-12 micrometer) camera that were set as co-axially as physically possible. The patient that was the subject of the thermal imaging is a 47 year-old white female with a recent histologically confirmed diagnosis of stage 0/1 ductal carcinoma in situ (DCIS) in the cranial-lateral quadrant of the right breast. At the time of the imaging she had received no form of therapy. Since IR cameras had different image formats it was obvious from Figure 1 that prior to applying LCNN blind de-mixing algorithm a proper registration, [26,27] of the multi-modality breast images had to be done. Generally, registration error was smaller for smaller images. Moreover, the asymmetry was common between two breasts. Therefore, the original images shown on Figure 1 had been segmented in two halves i.e. left breast and right breast images had been registered separately. Figure 2 showed mid IR and long IR images of the left breast after registration. The corresponding right breast images were shown on Figure 3. Vertical and horizontal labels represented pixel locations. It could be observed from both Figure 2 and Figure 3 that nipples on both left and right breast on mid and long wave IR images were located at the practically same pixel locations. This was not the case with the original images shown on Figure 1. We applied LCNN algorithm to sub-pixel de-mixing of the segmented and registered multispectral IR breast images with an unbiased and unsupervised detection of the pre-cancer anomaly heat generation. Figure 4 showed de-mixing results for the left breast while Figure 5 showed de-mixing results for the right breast. On Figures 4 and 5 red color meant class of the high probability (close to 1), while blue color meant class of low probability (close to 0) for absence of the class. The independent classes of the left breast shown on Figure 4 represented normal thermal

diffusive heat from large blood vessels inside of the breast. De-mixed right breast data into benign & malign pixels were shown on the Figure 5. The right upper part near the nipple, marked with the cyan circle, had a broken ring of red dots (about millimeter size each) and extended outside quadrant which shared the same capillary blood heat supply. Because the physiology of the breast suggested no existence of such heat sources around the normal healthy nipple, those malign points should not be there unless a stage zero ductal carcinoma in situ (DCIS) [19]. Left top was benign class because large thermal heat came from the normal blood vessels. According to [19] around 83% of tumors were formed in the upper breast hemisphere. That gave strong indication that aforementioned region could be a DCIS. Tracking IR imaging history or histologically would tell the truth. Following same line of argumentation the left breast, shown on Figure 4, could be considered healthy because the texture representing blood heat supply comes all around the nipple without break in the texture continuity.

IV. CONCLUSION

Two color IR images registered properly could provide physician better breast cancer diagnosis. Application of the multi-spectral LCNN algorithm to two-color or more IR breast imageries had demonstrated possibility for early cancer detection. In order to do that we recommended a high-resolution, computerized two to three spectral color co-axial channel normalized IR imaging screen units. The LCNN algorithm provided unbiased visual clues for physician diagnosis. Note that this sub-pixel dotted ring feature in Fig. 5 was not present in the raw infrared imageries Fig. 1. This was another value added by LCNN algorithm. Furthermore, the value added was that any isolated red dot called for the need of frequent non-intrusive passive imaging tracking by multiple infrared spectral images. This embodiment of multispectral smart neural network algorithm breast imaging was instantaneous, convenient, without and radiation hazard.

REFERENCES

- [1] K. Lloyd-Williams, and R. S. Handley, "Infra-red thermometry in the diagnosis of breast disease," *Lancet* 2, pp. 1378-1381, 1961.
- [2] R. S. Handley, "The temperature of breast tumors as a possible guide to prognosis," *Acta Unio Int Contra Cancrum* 18, 822, 1962.
- [3] R. N. Lawson, and M. S. Chughtai, "Breast cancer and body temperatures," *Can Med Assoc J* 88, pp. 68-70, 1963.
- [4] Gershen-Cohen J, Haberman J, and Brueschke EE: Medical thermography: A summary of current status. *Radiol Clin North Am* 3:403-431, 1965.
- [5] Haberman J: The present status of mammary thermography. In: *Ca - A Cancer Journal for Clinicians* 18: 314-321, 1968.
- [6] Jones C. H. Thermography of the female breast. In: Parsons CA (Ed): *Diagnosis of Breast Disease*. Baltimore: University Park Press, pp. 214-234, 1983.
- [7] Isard HJ, Becker W, Shilo R, et al.: Breast thermography after four years and 10,000 studies. *Am J Roentgenol* 115: 811-821, 1972.
- [8] Dodd GD: Thermography in breast cancer diagnosis. In *Abstracts for the Seventh National Cancer ConfProc*. Los Angeles, CA, Sept. 27-29, 1972. Toronto: Lippincott p. 267, 1972.
- [9] Wallace JD: Thermographic examination of the breast: An assessment of its present capabilities. In: Gallagher HS (Ed): *Early Breast Cancer: Detection and Treatment*. New York: Wiley, pp, 13-19, 1975.

[10] Stark A: The use of thermovision in the detection of early breast cancer. *Cancer* 33:1664-1670, 1964.

[11] Moskowitz M: Breast imaging. In: Donegan WL, Spratt IS (Eds): *Cancer of the Breast*. New York: Saunders, pp. 206-239, 1995.

[12] Head JF, Wang F, and Elliott RL: Breast thermography is a noninvasive prognostic procedure that predicts tumor growth rate in breast cancer patients. *Ann NYAcad Sci* 698:153-158, 1993.

[13] Read JF and Elliott RL: Breast thermography. *Cancer* 79:186-188, 1995.

[14] Gamagami P: Indirect signs of breast cancer: Angiogenesis study. In: *Atlas of Mammography*, Cambridge, MA: Blackwell Science, pp. 231-258, 1996.

[15] Guidi AJ and Schnitt SJ: Angiogenesis in preinvasive lesions of the breast. *The Breast J* 2: 364-369, 1996.

[16] Anbar M: Hyperthermia of the cancerous breast: Analysis of mechanism. *Cancer Lett* 84: 23-29, 1994.

[17] Anbar M: Breast cancer. In: *Quantitative Dynamic Telethermometry in Medical Diagnosis and Management*. Ann Arbor, MI: CRC Press, pp. 84-94, 1994.

[18] J.R. Keyserlink, P.D. Ahlgren, E. Yu, N. Belliveau, M. Yassa, "Functional Infrared Imaging of the breast," *Journal of IEEE Engineering in Medicine and Biology*, pp 30-41, May/June, 2000.

[19] Ch. Gorman, Rethinking Breast Cancer, *TIME*, pp. 50-58, February 18, 2002.

[20] H. Qi, P. T. Kuruganti, and Z. Li, "Early Detection of Breast Cancer using Thermal Texture Maps," submitted to 2002 IEEE International

Symposium on Biomedical Imaging Micro to Nano, Washington D.C., July 7-10, 2002.

[21] R. Balcerak, D. P. Jenkins, N. A. Diakides, Uncooled Infrared Focal Plane Arrays, Proc. 18th Annual Inter. Conference of the IEEE Engineering in Medicine and Biology Society, pp. 2077-2078, Amsterdam, 1996.

[22] B. F. Jones, "A Reappraisal of the Use of Infrared Thermal Image Analysis in Medicine," *IEEE Trans. On Medical Imaging*, pp. 1019-1027, vol. 17, No. 6, 1998.

[23] H. H. Szu and C. Hsu, Landsat spectral Unmixing à la superresolution of blind matrix inversion by constraint MaxEnt neural nets. *Proc. SPIE* 3078, pp.147-160, 1997.

[24] H.H.Szu, I.Kopriva, Comparison of the Lagrange Constrained Neural Network with Traditional ICA Methods, special session on Advancement in ICA, World Congress Computational Intelligence, Hawaii, USA, May 17-22, 2002.

[25] H. H. Szu, I. Kopriva, Constrained Equal a Priori Entropy for Unsupervised Remote Sensing, submitted to *IEEE Trans. Geosc. Remote Sensing*.

[26] H. H. Szu, "MO Imagery Techniques Using Arrays of Large Aperture Telescopes," *Optics Communications*, Vol. 32, No. 2, pp. 229-234, 1980.

[27] Map Tools in *ENVI User's Guide Version 3.4*, September 2000, Research Systems, Inc.

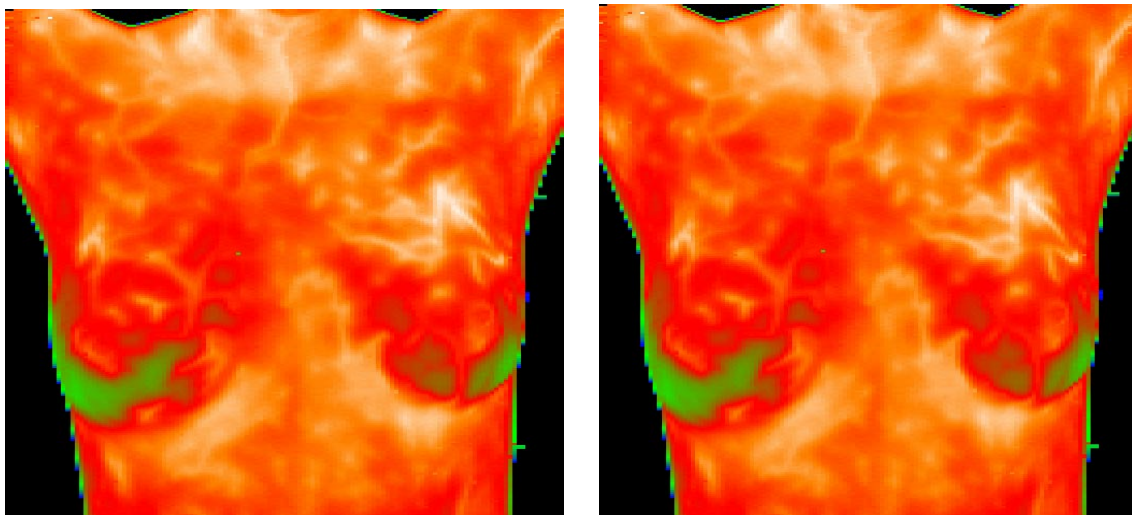


Figure 1. The mid IR (left) and long IR (right) breast images

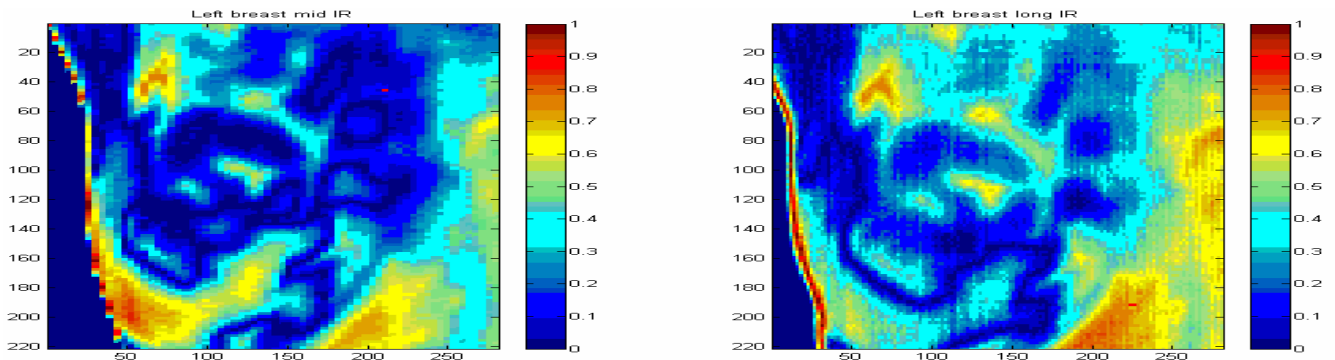


Figure 2. Registered mid IR (left) and long IR (right) images of the left breast. Red means high intensity.

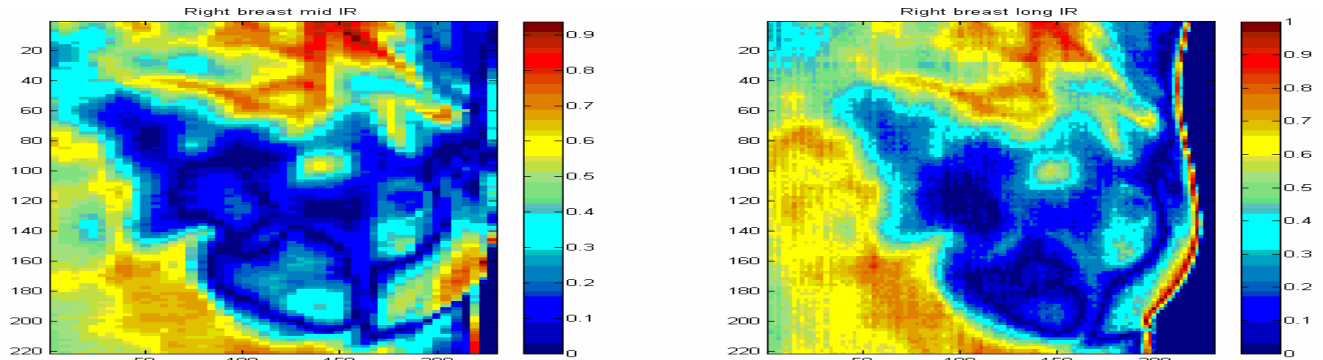


Figure 3. Registered mid IR (left) and long IR (right) images of the right breast. Red means high intensity.

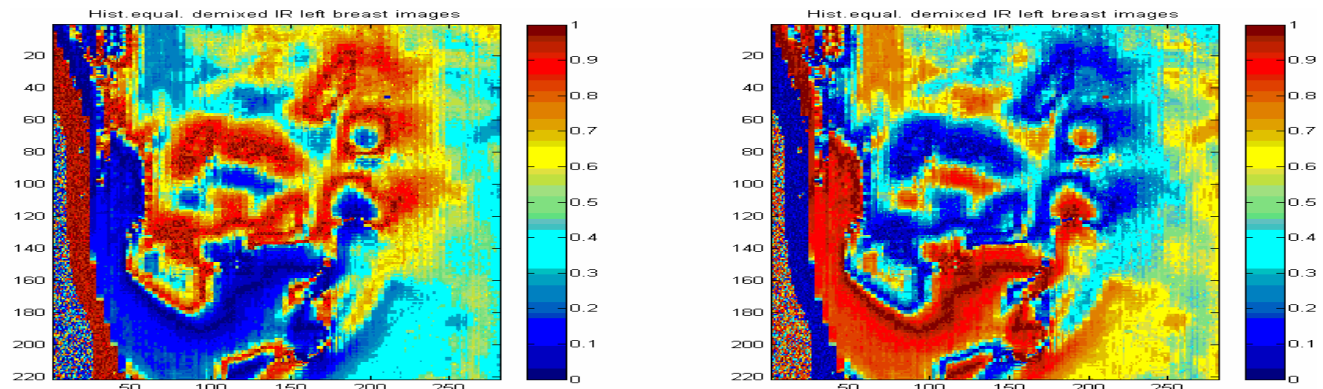


Figure 4. LCNN de-mixed images of the left breast. Red means class of high probability (1) and blue means class of low probability (0). Independent classes represent good thermal classes since most large heat classes come from the inside of the breast.

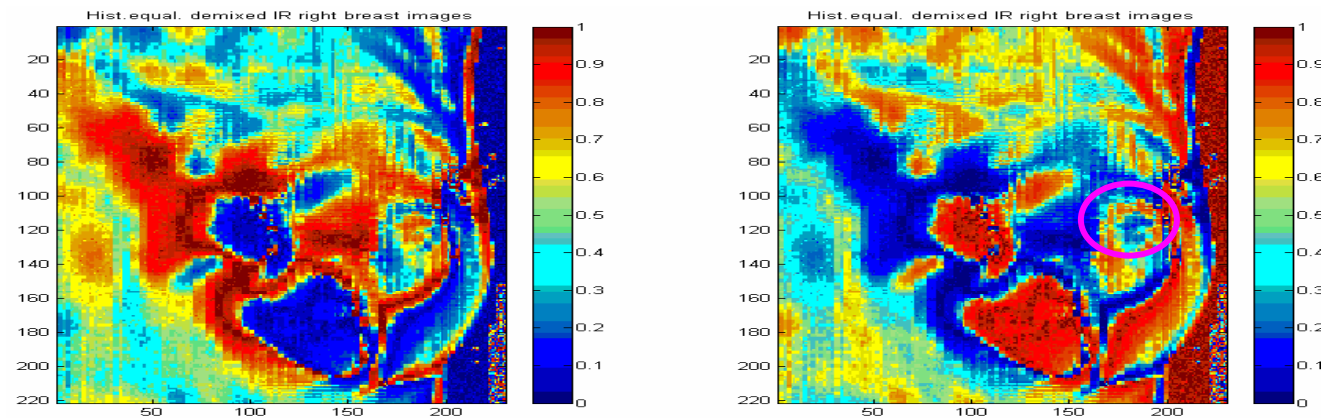


Figure 5. LCNN de-mixed images of the right breast. Red means class of high probability (1) and blue means class of low probability (0). The broken ring of small red pixel dots less than milli-meter size each and connected right outside quadrant, marked with the cyan circle, sharing the same texture of capillary shallow blood heat supply as the rest but should not be there since the nipple did not usually have the abnormal characteristics unless a stage zero ductal carcinoma in situ (DCIS).